
DIET-SNN: Direct Input Encoding With Leakage and Threshold Optimization in Deep Spiking Neural Networks

Nitin Rathi

School of Electrical and Computer Engineering
Purdue University
West Lafayette, IN, USA
rathi2@purdue.edu

Kaushik Roy

School of Electrical and Computer Engineering
Purdue University
West Lafayette, IN, USA
kaushik@purdue.edu

Abstract

Bio-inspired spiking neural networks (SNNs), operating with asynchronous binary signals (or spikes) distributed over time, can potentially lead to greater computational efficiency on event-driven hardware. The state-of-the-art SNNs suffer from high inference latency, resulting from inefficient input encoding, and sub-optimal settings of the neuron parameters (firing threshold, and membrane leak). We propose DIET-SNN, a low latency deep spiking network that is trained with gradient descent to optimize the membrane leak and the firing threshold along with other network parameters (weights). The membrane leak and threshold for each layer of the SNN are optimized with end-to-end backpropagation to achieve competitive accuracy at reduced latency. The analog pixel values of an image are directly applied to the input layer of DIET-SNN without the need to convert to spike-train. The information is converted into spikes in the first convolutional layer where leaky-integrate-and-fire (LIF) neurons integrate the weighted inputs and generate an output spike when the membrane potential crosses the trained firing threshold. The trained membrane leak controls the flow of input information and attenuates irrelevant inputs to increase the activation sparsity in the convolutional and linear layers of the network. The reduced latency combined with high activation sparsity provides large improvements in computational efficiency. We evaluate DIET-SNN on image classification tasks from CIFAR and ImageNet datasets on VGG and ResNet architectures. We achieve top-1 accuracy of 66.52% with 25 timesteps (inference latency) on the ImageNet dataset with $3.1\times$ less compute energy than an equivalent standard ANN. Additionally, DIET-SNN performs $5 - 100\times$ faster inference compared to other state-of-the-art SNN models.

1 Introduction

In recent years, a class of neural networks inspired by the event-driven form of computations in brain, has gained popularity for their promise of low-power computing [1, 2]. Spiking neural networks (SNNs) first emerged in computational neuroscience as an attempt to model the behavior of

biological neurons [3]. They were pursued for low-complexity tasks implemented on bio-plausible neuromorphic platforms. On the other hand in standard deep learning, the analog-valued artificial neural networks (ANNs) became the de-facto model for training various computer vision and natural language processing tasks [4, 5]. The skyrocketing performance and success of multi-layer ANNs came at a huge power and energy cost [6]. Recently, major chip maker Nvidia estimated that 80 – 90% of the energy cost of neural networks at data centers lies in inference processing [7]. The tremendous energy costs and the demand for edge intelligence on battery-powered devices have shifted the focus on exploring lightweight energy-efficient inference models for machine intelligence. To that effect, various techniques such as weight pruning [8], model compression [9], and quantization methods [10] have been proposed to reduce the size and computations in ANNs. Nonetheless, the inherent processing of analog values in ANNs requires expensive operation of multiplying two real numbers (except when both weights and activations are quantized to 1-bit [11]). In contrast, SNNs inherently compute and transmit information with binary signals providing a promising alternative for power-efficient machine intelligence. The computations in SNNs are performed with spikes (binary signals) distributed over time unlike one-shot analog computation in ANNs.

For a long time, the success of SNNs was delayed due to the unavailability of good learning algorithms. But in recent years, the advent of supervised learning algorithms for SNN has overcome many of the roadblocks surrounding the discontinuous derivative of spike activation function. Since SNNs receive and transmit information through spikes, analog values need to be encoded into spikes. There are a plethora of input encoding methods like rate coding [12, 13], temporal coding [14], rank-order coding [15], and other special coding schemes [16]. Also, dynamic vision sensors (DVS) record the change in image pixel intensities and directly convert it to spikes. Among these, rate-coding has shown competitive performance on complex tasks [12, 13, 17] while others have been limited to simple tasks like learning the XOR function and MNIST digit classification. The application of DVS data has been used to estimate optical flow [18] and classify hand gestures [19]. In rate coding, the analog value is encoded as the rate of firing of the neuron. In each timestep the neuron can either fire (output ‘1’) or stay inactive (output ‘0’). The length of timesteps¹ determines the discretization error in the representation of the analog value by spike-train. This leads to adopting a large number of timesteps for high accuracy at the expense of high inference latency [13]. The two other parameters that are crucial for SNNs are firing *threshold* of the neuron and membrane potential *leak*. The neuron fires when the membrane potential exceeds the firing threshold and the potential is reset after each firing. Such neurons are usually referred to as integrate-and-fire (IF) neurons. The threshold value is very significant for the correct operation of SNNs because a high threshold will prevent the neuron from firing (‘dead-neuron’ problem) and a lower threshold will lead to unnecessary firing, affecting the ability of the neuron to differentiate between two input patterns. Another neuron model introduces a leak factor that allows the membrane potential to keep decreasing over time. They are termed leaky-integrate-and-fire (LIF) neurons. Most of the recent work on supervised learning in SNNs have either employed the IF or the LIF neuron model [12, 13, 17, 21, 22]. There are some proposals that adopt kernel-based spike response models [23, 24], but for the most part, these approaches show limited performance on simple datasets and do not scale for deep networks. The leak parameter provides an additional knob that can potentially be used to tune SNNs for better energy-efficiency. However, there has not been any exploration of the full design space of optimizing the leak and the threshold to achieve better latency (or energy) and accuracy tradeoff. Research, so far, has been mainly focused on using fixed leak for the entire network and that can limit the capabilities of SNNs [17, 21]. The firing thresholds are also fixed [17] or selected based on some heuristics [13, 25]. In [13], the threshold was selected as the maximum pre-activation of each layer, whereas in [25] the authors selected a certain percentile of the pre-activation distribution as the threshold. The current challenges in SNN models are high inference latency and energy, long training time, and high training cost in terms of memory and computation. Most of these challenges arise due to in-efficient input encoding, and improper methods of selecting the membrane leak and the threshold.

To address these challenges, this paper makes the following contributions:

- We propose a gradient descent based training method that learns the correct membrane leak and firing threshold for each layer of a deep spiking network via error-backpropagation. The goal is to jointly optimize the neuron parameters (membrane leak and threshold) and the network parameters (weights) to achieve high accuracy at low inference latency. The

¹The actual real time for one ‘timestep’ is dependent on the number of computations performed and the underlying hardware [20]. In simulation, one timestep is the time taken to perform one forward pass

tailored membrane leak and threshold for each layer leads to large improvement in activation sparsity and energy-efficiency.

- We train the first convolutional layer to act as the spike-generator, whose spike-rate is a function of the weights, membrane leak, and threshold. This also eliminates the need for a generator function (and associated overheads) used in other coding schemes².
- To evaluate the effectiveness of the proposed algorithm, we train SNNs on both VGG [26] and ResNet [27] architectures for CIFAR [28] and ImageNet [29] datasets. DIET-SNN achieves similar accuracy as ANN with $2 - 8\times$ less compute energy. The performance is achieved at inference latency of $20 - 25$ timesteps compared to $100 - 2000$ timesteps for state-of-the-art SNN models.

The source code implemented in Pytorch framework is available in the supplementary materials.

2 Background and Related Work

The development of efficient learning algorithms for deep SNNs is an on-going research challenge. There has been good amount of success with recent supervised learning algorithms [30, 31, 13, 32, 22] that can be broadly classified as conversion algorithms [33, 25, 13] and spike-based backpropagation algorithms [30, 17]. There are also some variants of bio-plausible algorithms that employ feedback alignment to update the weights. These algorithms apply random weights [34] or fixed weights [35] as the feedback weight during backpropagation³. The success of these algorithms has been limited to simple tasks. Therefore, we focus our discussion on ANN-SNN conversion and backpropagation algorithms that are more suitable for complex tasks and are scalable to deep network architectures.

ANN-SNN Conversion: ANN-SNN conversion is the most successful method of training rate-coded deep SNNs [33, 12, 25, 13, 22]. In this process, an ANN with ReLU neurons is trained with standard backpropagation with some restrictions (no bias, average pooling, no batch normalization), although some works have shown that some of the restrictions can be relaxed [25]. The weights of the trained ANN are then transferred to an SNN implemented in the corresponding network architecture with IF neurons. The underlying principle of this process is that a ReLU neuron can be mapped to an IF neuron with minimum loss. The mapping is possible for SNNs that operate on rate-coded inputs [12, 13] or on direct input encoding [25]. The major bottleneck of this method is to determine the firing threshold of the IF neurons that can balance the accuracy-latency tradeoff. Generally, the threshold is computed as the maximum pre-activation of the IF neuron resulting in high inference accuracy at the cost of high inference latency ($2000 - 2500$ timesteps) [13]. In recent work, the authors showed that instead of using the maximum pre-activation, a certain percentile of the pre-activation distribution reduces the inference latency ($100 - 200$ timesteps) with minimal accuracy drop [36]. These heuristic techniques of determining the firing threshold lead to a sub-optimal accuracy-latency tradeoff. Additionally, ANN-SNN conversion has a major drawback: the absence of the timing information. The quintessential parameter ‘time’ is not utilized in the conversion process which leads to higher inference latency.

Error Backpropagation in SNN: ANNs have achieved good success with gradient-based training that backpropagates the error signal from the output layer to the input layer. This requires computing a gradient of each operation performed in the forward pass. Unfortunately, the IF and the LIF neuron does not have a continuous gradient. The gradient of the spike function (Dirac delta) is undefined at the time of spike and zero otherwise. This has hindered the application of standard backpropagation in SNN. There have been many proposals to perform gradient-based training in SNNs [23, 17] – among them the most successful is surrogate-gradient based optimization [37]. The real discontinuous gradient of the IF neuron is approximated by a continuous function that serves as the surrogate for the real gradient. SNNs trained with surrogate-gradient perform backpropagation through time (BPTT) to achieve high accuracy and low latency (100 timesteps), but the training is very compute and memory intensive in terms of total training iterations compared to conversion techniques. The multiple-iteration training effort with exploding memory requirement for backpropagation has limited the application of this method to simpler tasks on shallow architectures [17].

²For rate-coding, a Poisson generator is used to convert the analog values to spike-train [12]. The encoder generates random numbers every timestep and compares it with the analog values to produce the spikes.

³In standard backpropagation the feedback weight is W^T , where W is the weight matrix used in the forward pass

Hybrid SNN Training: In recent work, the authors proposed a hybrid mechanism to circumvent the high training costs of backpropagation and at the same time maintain low inference latency (100 – 250 timesteps) [21]. The technique involves both ANN-SNN conversion and error-backpropagation. First, a trained ANN is converted to an SNN as described earlier. The weights of the converted SNN are further fine-tuned with surrogate gradient and BPTT. The authors showed a faster convergence (< 20 epochs) in SNN training due to the precursory initialization from the ANN-SNN conversion. This enables the training of deep SNNs practically feasible with limited resources that is otherwise difficult with only backpropagation from random initialization [17]. Hybrid training tries to achieve the best of both worlds: high accuracy and low latency. But it still employs rate coding, and the membrane leak and threshold are fixed and therefore, the latency-accuracy tradeoff can still be improved.

In this work, we adopt the hybrid training method to train the SNNs. We start with ANN-SNN conversion and select the threshold for each layer as 99.7 percentile of the pre-activation distribution. The membrane leak is set to unity. The pixel intensities are directly applied in the input layer during the threshold selection. This serves as the initial model that is further trained to optimize the membrane leak and threshold in each layer with BPTT.

3 Algorithm for training DIET-SNN

Direct Input Encoding: The pixel intensities of an image are applied directly to the input layer of the SNN at each timestep [25, 36]. The first convolutional layer composed of LIF neurons acts as both the feature extractor and the spike-generator, which accumulates the weighted pixel values and generates output spikes. This is similar to rate-coding but the spike-rate is a function of the weights, membrane leak and threshold that are learned by training.

Neuron Model: We employ the LIF neuron model described by

$$u_i^t = \lambda_i u_i^{t-1} + \sum_j w_{ij} o_j^t - v_i o_i^{t-1} \quad (1)$$

$$z_i^{t-1} = \frac{u_i^{t-1}}{v_i} - 1 \quad \text{and} \quad o_i^{t-1} = \begin{cases} 1, & \text{if } z_i^{t-1} > 0 \\ 0, & \text{otherwise} \end{cases} \quad (2)$$

where u is the membrane potential, λ is the leak factor with a value in $[0 - 1]$, w is the weight connecting pre-neuron j and post-neuron i , o is the binary spike output, v is the firing threshold, and t represents the timestep. The first term in Equation 1 denotes the leakage in the membrane potential, the second term integrates the weighted input received from pre-neuron, and the third term accounts for the reduction in potential when the neuron generates an output spike. We reduce the potential by the same amount as threshold instead of resetting it to zero at the time of the spike [22]. The threshold governs the average integration time of input, and the leak regulates how much of the potential is retained from the previous timestep. The three parameters: weight, leak, and threshold must be jointly optimized to achieve the best accuracy-latency tradeoff. Let us derive the expressions required to backpropagate the error from the output layer to the input layer and compute the gradients of the parameters at all intermediate layers. The spatial and temporal credit assignment is performed by unrolling the network in time and employing BPTT.

Output layer: The neuron model in the output layer only accumulates the incoming inputs without any leakage and does not generate an output spike and is described by

$$U_l^t = U_l^{t-1} + W_l O_{l-1}^t \quad (3)$$

where U_l is a vector containing membrane potential of N output neurons, N is the number of classes in the task, W_l is the weight matrix connecting the output layer and the previous layer, and O_{l-1} is a vector containing the spike signals from layer $(l - 1)$. The loss function is defined on U_l at the last timestep T . We employ the cross-entropy loss and the softmax is computed on U_l^T . The symbol T is

used for timestep and not to denote the transpose of a matrix.

$$S(U_l^T) : \begin{bmatrix} u_1^T \\ \dots \\ u_N^T \end{bmatrix} \rightarrow \begin{bmatrix} s_1 \\ \dots \\ s_N \end{bmatrix} \quad s_i = \frac{e^{u_i^T}}{\sum_{k=1}^N e^{u_k^T}} \quad (4)$$

$$L = - \sum_i y_i \log(s_i) \quad (5)$$

$$\frac{\partial L}{\partial U_l^T} = S - Y \quad (6)$$

where S is the vector containing the softmax values, L is the loss function, Y is the one-hot encoded vector of the true label or target. The weight update is computed as

$$W_l = W_l - \eta \Delta W_l \quad (7)$$

$$\Delta W_l = \sum_t \frac{\partial L}{\partial W_l} = \sum_t \frac{\partial L}{\partial U_l^t} \frac{\partial U_l^t}{\partial W_l} = \frac{\partial L}{\partial U_l^T} \sum_t \frac{\partial U_l^t}{\partial W_l} = (S - Y) \sum_t O_{l-1}^t \quad (8)$$

$$\frac{\partial L}{\partial O_{l-1}^t} = \frac{\partial L}{\partial U_l^T} \frac{\partial U_l^t}{\partial O_{l-1}^t} = (S - Y) W_l \quad (9)$$

where η is the learning rate.

Hidden layers: The neurons in the convolutional and linear layers are defined by the LIF model as

$$U_l^t = \Lambda_l U_l^{t-1} + W_l O_{l-1}^t - V_l O_l^{t-1} \quad (10)$$

$$Z_l^t = \frac{U_l^t}{V_l} - 1 \quad \text{and} \quad O_l^t = \begin{cases} 1, & \text{if } Z_l^t > 0 \\ 0, & \text{otherwise} \end{cases} \quad (11)$$

where $\Lambda(V)$ is a single real value representing leak (threshold) for all neurons in layer l . All neurons in a layer share the same leak and threshold value. This reduces the number of trainable parameters and we did not observe any significant improvement by assigning individual threshold/leak to each neuron. The weight update is calculated as

$$\Delta W_l = \sum_t \frac{\partial L}{\partial W_l} = \sum_t \frac{\partial L}{\partial O_l^t} \frac{\partial O_l^t}{\partial Z_l^t} \frac{\partial Z_l^t}{\partial U_l^t} \frac{\partial U_l^t}{\partial W_l} = \sum_t \frac{\partial L}{\partial O_l^t} \frac{\partial O_l^t}{\partial Z_l^t} \frac{1}{V_l} O_{l-1}^t \quad (12)$$

$\partial O_l^t / \partial Z_l^t$ is the discontinuous gradient and we approximate it with the surrogate gradient [30]

$$\frac{\partial O_l^t}{\partial Z_l^t} = \gamma \max\{0, 1 - |Z_l^t|\} \quad \text{and} \quad \frac{\partial O_l^t}{\partial U_l^t} = \frac{\partial O_l^t}{\partial Z_l^t} \frac{\partial Z_l^t}{\partial U_l^t} = \frac{\partial O_l^t}{\partial Z_l^t} \frac{1}{V_l} \quad (13)$$

where γ is a constant denoting the maximum value of the gradient. The threshold update is then computed as

$$V_l = V_l - \eta \Delta V_l \quad (14)$$

$$\Delta V_l = \sum_t \frac{\partial L}{\partial V_l} = \sum_t \frac{\partial L}{\partial O_l^t} \frac{\partial O_l^t}{\partial Z_l^t} \frac{\partial Z_l^t}{\partial V_l} = \sum_t \frac{\partial L}{\partial O_l^t} \frac{\partial O_l^t}{\partial Z_l^t} \left(\frac{V_l (-O_l^{t-1}) - U_l^t}{(V_l^2)} \right) \quad (15)$$

And finally the leak update is computed as

$$\Lambda_l = \Lambda_l - \eta \Delta \Lambda_l \quad \text{and} \quad \Delta \Lambda_l = \sum_t \frac{\partial L}{\partial \Lambda_l} = \sum_t \frac{\partial L}{\partial O_l^t} \frac{\partial O_l^t}{\partial U_l^t} \frac{\partial U_l^t}{\partial \Lambda_l} = \sum_t \frac{\partial L}{\partial O_l^t} \frac{\partial O_l^t}{\partial U_l^t} U_l^{t-1} \quad (16)$$

4 Experiments

Table 1: Top-1 classification accuracy

Architecture	ANN	DIET-SNN	Timesteps
CIFAR10			
VGG6	90.80%	89.34%	15
VGG16	93.72%	92.64%	20
ResNet20	92.79%	92.14%	25
CIFAR100			
VGG16	71.82%	69.37%	20
ResNet20	64.64%	64.44%	25
ImageNet [†]			
VGG16	70.08%	66.52%	25

[†]after 2 epochs of SNN training, training was incomplete due to time and resource constraints. We expect the accuracy to increase and will have the final results at the time of rebuttal along with the results for ResNet

The three-step DIET-SNN training pipeline is shown in Fig. 1. First, we train an ANN with some restrictions to achieve minimal loss during the process of ANN-SNN conversion [12, 13, 21]. The neurons in the network do not have the bias term. Also note, batch-normalization is not employed because this helps in calculating the threshold during the conversion. Instead, Dropout [38] is used as the regularizer and the dropout mask is kept fixed for all timesteps [21]. Average-pooling is used to reduce the feature map size in VGG architectures at layers where the number of filters increase. In ResNet, a stride of 2 is employed in the convolution layer to reduce the feature map size. The complete architecture details, training hyperparameters, and dataset descriptions are provided in the supplementary section. Next, the trained ANN is converted to SNN with IF neurons. The threshold for each layer is computed sequentially as the 99.7 percentile of the pre-activation distribution at each layer [25, 36]. The pre-activation for each neuron is the weighted sum of inputs $\sum_j O_j W_{ij}$ received by the neuron. The threshold computation happens with IF neurons (leak=1) in the hidden layers and the input layer employs direct input encoding. Finally, the converted SNN is trained with error-backpropagation to optimize the weights, the membrane leak, and the firing thresholds of each layer as described by the equations in Section 3. We evaluated the performance of DIET-SNN on VGG and ResNet architectures for CIFAR and ImageNet datasets (Table 1). We additionally trained a VGG6 network without the hybrid approach and performed backpropagation training from random initialization and achieved 85.72% accuracy for CIFAR10 dataset with 20 timesteps in 225 epochs. This shows that the proposed optimization of the membrane leak and threshold works with random initialization as well. The hybrid approach is employed to speed up the training process and make the training of deep spiking networks practically viable. The performance of DIET-SNN compared to current state-of-the-art SNNs is shown in Table 2. DIET-SNN achieves comparable or better accuracy than the other methods at 5 – 100× lower number of timesteps (in other words, it achieves 5 – 100× improvement in inference latency). The authors in [32] employed a special input encoding layer to convert analog value to spikes, the implementation of that is not very clear. They achieved convergence in 12 timesteps but the overhead of the encoding layer may affect the overall energy.

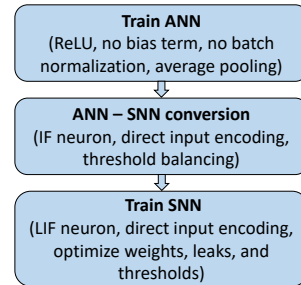


Figure 1: DIET-SNN training pipeline

5 Energy Efficiency

In ANN, each operation computes a dot-product involving one floating-point (FP) multiplication and one FP addition (MAC), whereas in SNN, each operation is only one FP addition due to binary spikes. The computations in SNN implemented on neuromorphic hardware are event-driven and occurs when there are spikes [2, 20]. In the absence of spikes, no computation occurs and therefore no active energy is consumed. We computed the energy cost/operation for ANNs and SNNs in standard CMOS technology (see (Table 3)). The energy cost for ANN MAC operation ($4.6pJ$) is $5.1\times$ more than

Table 2: DIET-SNN compared with other SNN models

Model	Method	Architecture	SNN Accuracy	Timesteps
CIFAR10				
Cao et al. [33]	ANN-SNN	3 Conv, 2 Linear	77.43%	400
Lee et al. [17]	Backprop	VGG9	90.45%	100
Wu et al. [32]	Backprop	5 Conv, 2 Linear	90.53%	12
Rueckauer et al. [25]	ANN-SNN	4 Conv, 2 Linear	90.85%	400
Sengupta et al. [13]	ANN-SNN	VGG16	91.55%	2500
Rathi et al. [21]	Hybrid	VGG16	92.02%	200
Han et al. [22]	ANN-SNN	VGG16	93.41%	768
This work	DIET-SNN	VGG16	92.64%	20
CIFAR100				
Lu and Sengupta [36]	ANN-SNN	VGG15	63.20%	62
Rathi et al. [21]	Hybrid	VGG11	67.87%	125
Han et al. [22]	ANN-SNN	VGG16	70.09%	768
This work	DIET-SNN	VGG16	69.37%	20
ImageNet				
Rueckauer et al. [25]	ANN-SNN	VGG16	49.61%	400
Rathi et al. [21]	Hybrid	VGG16	65.19%	250
Lu and Sengupta [36]	ANN-SNN	VGG15	66.56%	64
Sengupta et al. [13]	ANN-SNN	VGG16	69.96%	2500
Han et al. [22]	ANN-SNN	VGG16	71.34%	768
This work	DIET-SNN	VGG16	66.52%	25

SNN addition operation ($0.9pJ$). In ANN, the number of operations/layer is defined by

$$\#Operations_{ANN} = \begin{cases} K_w \times K_h \times C_{in} \times H_{out} \times W_{out} \times C_{out}, & \text{Convolution layer} \\ F_{in} \times F_{out}, & \text{Linear layer} \end{cases} \quad (17)$$

where $K_w(K_h)$ is kernel width (height), $C_{in}(C_{out})$ is the number of input (output) channels, $H_{out}(W_{out})$ is the height (width) of the output feature map, and $F_{in}(F_{out})$ is the number of input (output) features. The number of operations/layer in iso-architecture SNN is specified by

$$\#Operations_{SNN} = SpikeRate_l \times \#Operations_{ANN} \quad (18)$$

$$SpikeRate_l = \frac{\#TotalSpikes_l \text{ over all inference timesteps}}{\#Neurons_l} \quad (19)$$

where $SpikeRate_l$ is the total spikes in layer l over all timesteps averaged over the number of neurons in layer l . A spike rate of 1 indicates that each neuron fired once to classify one image and in this case the number of operations for ANN and SNN are the same. Lower spike rates denote more sparsity in spike events and higher energy-efficiency. The layerwise spike rate for VGG and ResNet architectures in DIET-SNN during inference is shown in Fig. 2. In each layer the spike rate is well below 5.1, indicating that DIET-SNN is more energy-efficient than ANN for every layer. In ResNet, the spike rate drops below 1 for the deeper layers and deep SNNs with residual connections can potentially be more energy-efficient. Table 4 shows the compute energy comparison of ANN and DIET-SNN for different settings of architecture and datasets. The energy for ResNet is more than VGG because more than 50% of the total operations in ResNet occurs in the first 3 layers where the spike rate is high. The standard ResNet architecture was modified with initial 3 plain conv layers to minimize the accuracy loss during ANN-SNN conversion [13]. The authors in [36] reported an average spike rate of 2.35 for VGG16 for CIFAR100 with 62% accuracy. The maximum spike rate of 20 was reported for VGG16 architecture with CIFAR10 dataset [21]. DIET-SNN performs

Table 4: ANN vs DIET-SNN compute energy. Each operation in ANN (SNN) consumes $4.6pJ$ ($0.9pJ$). The input layer in DIET-SNN is non-spiking, so its energy is same as ANN. Column-5 shows the ratio of #operations in input layer to the total #operations in the network.

Architecture (timesteps)	Dataset	Normalized $Ops_{ANN}(a)$	Normalized $Ops_{SNN}(b)$	$\frac{\#Ops_{layer\ 1}}{\text{Total } \#Ops}(c)$	ANN/DIET-SNN Energy $(\frac{a*4.6}{c*4.6+(1-c)*b*0.9})$
VGG6 (T=15)	CIFAR10	1.0	0.49	0.029	8.2
VGG16 (T=20)	CIFAR10	1.0	1.65	0.005	3.1
VGG16 (T=20)	CIFAR100	1.0	1.62	0.005	3.1
VGG16 (T=25)	ImageNet	1.0	1.62	0.006	3.1
ResNet20 (T=25)	CIFAR10	1.0	2.55	0.013	2.0
ResNet20 (T=25)	CIFAR100	1.0	2.28	0.013	2.2

considerably better in all metrics compared to these models and to the best of our knowledge this is the first spiking network to show better compute energy than ANN on complex tasks like CIFAR and ImageNet with similar accuracy. We did not consider the data movement cost in our evaluation as it is dependent on the system architecture and the underlying hardware implementation. Although we would like to mention that in SNN the membrane potentials have to be fetched at every timestep, in addition to the weights and activations. Many proposals reduce the memory cost by employing crossbar-based in-memory computations [40], trading computations for memory [41], and data reuse through efficient dataflows [42]. All such techniques can be extended to SNNs to address the memory cost. The training of SNNs is still a cause of concern for energy-efficiency because it requires several days, even on high-performance GPUs. The hybrid approach and DIET-SNN alleviate the issue by reducing the number of training epochs and the number of timesteps, but further innovations in both algorithms and accelerators for SNNs are required to reduce the training cost.

6 Conclusions

SNNs that operate with asynchronous discrete events can potentially solve the energy issue in deep learning. To that effect, we presented DIET-SNN, an energy-efficient spiking network that is trained to operate with low inference latency and high activation sparsity. The membrane leak and the firing threshold of the LIF neurons are trained with error-backpropagation along with the weights of the network to optimize both accuracy and latency. We initialize the parameters of DIET-SNN, taken from a trained ANN, to speed-up the training with spike-based backpropagation. The image pixels are applied directly as input to the network, and the first convolutional layer is trained to perform the spike-generation operation. This leads to high activation sparsity in the convolutional and linear layers of the network. The high sparsity combined with low inference latency reduces the compute energy by $2 - 8\times$ compared to an equivalent ANN with similar accuracy. DIET-SNN achieves similar accuracy as other state-of-the-art SNN models with $5 - 100\times$ less number of timesteps.

Table 3: Energy costs of addition and multiplication in 45nm CMOS [39]

FP ADD (32 bit)	$0.9pJ$
FP MULT (32 bit)	$3.7pJ$
FP MAC (32 bit)	$(0.9 + 3.7)$ $= 4.6pJ$

Acknowledgments and Disclosure of Funding

This work was supported in part by the National Science Foundation, Vannevar Bush Faculty Fellowship, Sandia National Laboratory, ONR MURI, and by the Center for Brain-Inspired Computing (C-BRIC), one of six centers in JUMP, funded by Semiconductor Research Corporation (SRC) and DARPA.

References

- [1] Eustace Painkras, Luis A Plana, Jim Garside, Steve Temple, Francesco Galluppi, Cameron Patterson, David R Lester, Andrew D Brown, and Steve B Furber. Spinnaker: A 1-w 18-core

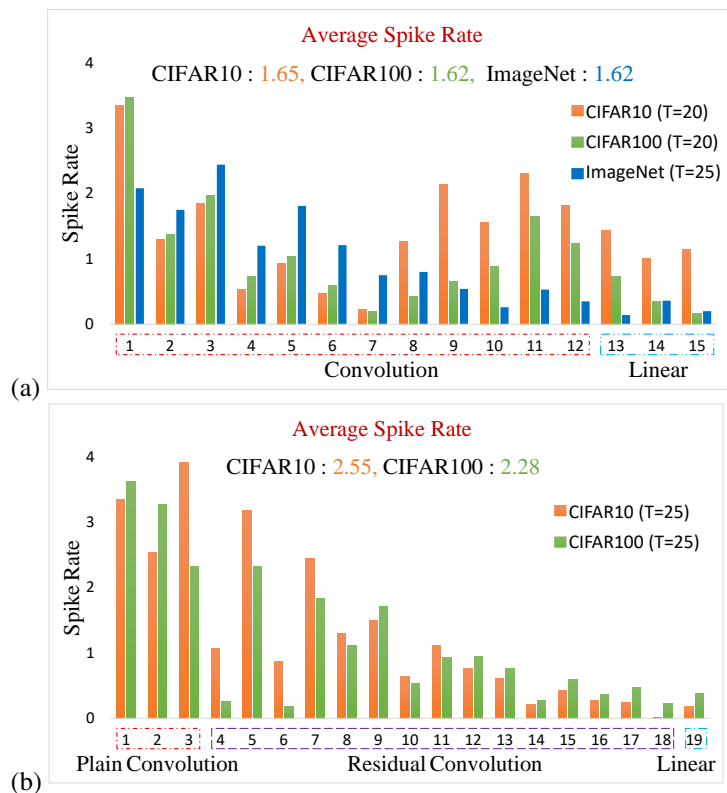


Figure 2: Layerwise spike rate for (a) VGG16, and (b) ResNet20 architecture in DIET-SNN during inference over entire test-set. Average spike rate is calculated as total number of spikes over total number of neurons in the network averaged over the entire test set. An average spike rate of 1.65 indicates that each neuron in the network fired on average 1.65 times for each image over the inference time window.

system-on-chip for massively-parallel neural network simulation. *IEEE Journal of Solid-State Circuits*, 48(8):1943–1953, 2013.

- [2] Mike Davies, Narayan Srinivasa, Tsung-Han Lin, Gautham China, Yongqiang Cao, Sri Harsha Choday, Georgios Dimou, Prasad Joshi, Nabil Imam, Shweta Jain, et al. Loihi: A neuromorphic manycore processor with on-chip learning. *IEEE Micro*, 38(1):82–99, 2018.
- [3] Zachary F Mainen and Terrence J Sejnowski. Reliability of spike timing in neocortical neurons. *Science*, 268(5216):1503–1506, 1995.
- [4] Alex Krizhevsky, Ilya Sutskever, and Geoffrey E Hinton. Imagenet classification with deep convolutional neural networks. In *Advances in neural information processing systems*, pages 1097–1105, 2012.
- [5] Geoffrey Hinton, Li Deng, Dong Yu, George E Dahl, Abdel-rahman Mohamed, Navdeep Jaitly, Andrew Senior, Vincent Vanhoucke, Patrick Nguyen, Tara N Sainath, et al. Deep neural networks for acoustic modeling in speech recognition: The shared views of four research groups. *IEEE Signal processing magazine*, 29(6):82–97, 2012.
- [6] Da Li, Xinbo Chen, Michela Becchi, and Ziliang Zong. Evaluating the energy efficiency of deep convolutional neural networks on cpus and gpus. In *2016 IEEE International Conferences on Big Data and Cloud Computing (BDCloud), Social Computing and Networking (SocialCom), Sustainable Computing and Communications (SustainCom)(BDCloud-SocialCom-SustainCom)*, pages 477–484. IEEE, 2016.
- [7] Karl Freund. Google cloud doubles down on nvidia gpus for inference, 2019. URL <https://www.forbes.com/sites/moorinsights/2019/05/09/google-cloud-doubles-down-on-nvidia-gpus-for-inference/#745312fe6792>.

- [8] Song Han, Huizi Mao, and William J Dally. Deep compression: Compressing deep neural networks with pruning, trained quantization and huffman coding. *arXiv preprint arXiv:1510.00149*, 2015.
- [9] Yihui He, Ji Lin, Zhijian Liu, Hanrui Wang, Li-Jia Li, and Song Han. Amc: Automl for model compression and acceleration on mobile devices. In *Proceedings of the European Conference on Computer Vision (ECCV)*, pages 784–800, 2018.
- [10] Indranil Chakraborty, Deboleena Roy, Isha Garg, Aayush Ankit, and Kaushik Roy. Constructing energy-efficient mixed-precision neural networks through principal component analysis for edge intelligence. *Nature Machine Intelligence*, pages 1–13, 2020.
- [11] Mohammad Rastegari, Vicente Ordonez, Joseph Redmon, and Ali Farhadi. Xnor-net: Imagenet classification using binary convolutional neural networks. In *European conference on computer vision*, pages 525–542. Springer, 2016.
- [12] Peter U Diehl, Daniel Neil, Jonathan Binas, Matthew Cook, Shih-Chii Liu, and Michael Pfeiffer. Fast-classifying, high-accuracy spiking deep networks through weight and threshold balancing. In *2015 International Joint Conference on Neural Networks (IJCNN)*, pages 1–8. IEEE, 2015.
- [13] Abhronil Sengupta, Yuting Ye, Robert Wang, Chiao Liu, and Kaushik Roy. Going deeper in spiking neural networks: Vgg and residual architectures. *Frontiers in neuroscience*, 13, 2019.
- [14] Iulia M Comsa, Thomas Fischbacher, Krzysztof Potempa, Andrea Gesmundo, Luca Versari, and Jyrki Alakuijala. Temporal coding in spiking neural networks with alpha synaptic function. In *ICASSP 2020-2020 IEEE International Conference on Acoustics, Speech and Signal Processing (ICASSP)*, pages 8529–8533. IEEE, 2020.
- [15] Saeed Reza Kheradpisheh and Timothee Masquelier. Temporal backpropagation for spiking neural networks with one spike per neuron. *International Journal of Neural Systems*, 2020.
- [16] Ammar Almomani, Mohammad Alauthman, Mohammed Alweshah, O Dorgham, and Firas Albalas. A comparative study on spiking neural network encoding schema: implemented with cloud computing. *Cluster Computing*, 22(2):419–433, 2019.
- [17] Chankyu Lee, Syed Shakib Sarwar, and Kaushik Roy. Enabling spike-based backpropagation in state-of-the-art deep neural network architectures. *arXiv preprint arXiv:1903.06379*, 2019.
- [18] Chankyu Lee, Adarsh Kosta, Alex Zihao Zhu, Kenneth Chaney, Kostas Daniilidis, and Kaushik Roy. Spike-flownet: Event-based optical flow estimation with energy-efficient hybrid neural networks. *arXiv preprint arXiv:2003.06696*, 2020.
- [19] Sumit Bam Shrestha and Garrick Orchard. Slayer: Spike layer error reassignment in time. In *Advances in Neural Information Processing Systems*, pages 1412–1421, 2018.
- [20] E Paxon Frady, Garrick Orchard, David Florey, Nabil Imam, Ruokun Liu, Joyesh Mishra, Jonathan Tse, Andreas Wild, Friedrich T Sommer, and Mike Davies. Neuromorphic nearest-neighbor search using intel’s pohoiki springs. *arXiv preprint arXiv:2004.12691*, 2020.
- [21] Nitin Rathi, Gopalakrishnan Srinivasan, Priyadarshini Panda, and Kaushik Roy. Enabling deep spiking neural networks with hybrid conversion and spike timing dependent backpropagation. In *International Conference on Learning Representations*, 2020. URL <https://openreview.net/forum?id=B1xSperKvH>.
- [22] Bing Han, Gopalakrishnan Srinivasan, and Kaushik Roy. Rmp-snns: Residual membrane potential neuron for enabling deeper high-accuracy and low-latency spiking neural networks. In *The IEEE Conference on Computer Vision and Pattern Recognition (CVPR)*, June 2020.
- [23] Dongsung Huh and Terrence J Sejnowski. Gradient descent for spiking neural networks. In *Advances in Neural Information Processing Systems*, pages 1433–1443, 2018.
- [24] Sander M Bohte, Joost N Kok, and Johannes A La Poutré. Spikeprop: backpropagation for networks of spiking neurons. In *ESANN*, pages 419–424, 2000.

- [25] Bodo Rueckauer, Iulia-Alexandra Lungu, Yuhuang Hu, Michael Pfeiffer, and Shih-Chii Liu. Conversion of continuous-valued deep networks to efficient event-driven networks for image classification. *Frontiers in neuroscience*, 11:682, 2017.
- [26] Karen Simonyan and Andrew Zisserman. Very deep convolutional networks for large-scale image recognition. *arXiv preprint arXiv:1409.1556*, 2014.
- [27] Kaiming He, Xiangyu Zhang, Shaoqing Ren, and Jian Sun. Deep residual learning for image recognition. In *Proceedings of the IEEE conference on computer vision and pattern recognition*, pages 770–778, 2016.
- [28] Alex Krizhevsky, Geoffrey Hinton, et al. Learning multiple layers of features from tiny images. Technical report, Citeseer, 2009.
- [29] Jia Deng, Wei Dong, Richard Socher, Li-Jia Li, Kai Li, and Li Fei-Fei. Imagenet: A large-scale hierarchical image database. In *2009 IEEE conference on computer vision and pattern recognition*, pages 248–255. Ieee, 2009.
- [30] Guillaume Bellec, Darjan Salaj, Anand Subramoney, Robert Legenstein, and Wolfgang Maass. Long short-term memory and learning-to-learn in networks of spiking neurons. In *Advances in Neural Information Processing Systems*, pages 787–797, 2018.
- [31] Yujie Wu, Lei Deng, Guoqi Li, Jun Zhu, and Luping Shi. Spatio-temporal backpropagation for training high-performance spiking neural networks. *Frontiers in neuroscience*, 12, 2018.
- [32] Yujie Wu, Lei Deng, Guoqi Li, Jun Zhu, Yuan Xie, and Luping Shi. Direct training for spiking neural networks: Faster, larger, better. In *Proceedings of the AAAI Conference on Artificial Intelligence*, volume 33, pages 1311–1318, 2019.
- [33] Yongqiang Cao, Yang Chen, and Deepak Khosla. Spiking deep convolutional neural networks for energy-efficient object recognition. *International Journal of Computer Vision*, 113(1):54–66, 2015.
- [34] Timothy P Lillicrap, Daniel Cownden, Douglas B Tweed, and Colin J Akerman. Random synaptic feedback weights support error backpropagation for deep learning. *Nature communications*, 7(1):1–10, 2016.
- [35] Arash Samadi, Timothy P Lillicrap, and Douglas B Tweed. Deep learning with dynamic spiking neurons and fixed feedback weights. *Neural computation*, 29(3):578–602, 2017.
- [36] Sen Lu and Abhronil Sengupta. Exploring the connection between binary and spiking neural networks. *arXiv preprint arXiv:2002.10064*, 2020.
- [37] Emre O Neftci, Hesham Mostafa, and Friedemann Zenke. Surrogate gradient learning in spiking neural networks. *arXiv preprint arXiv:1901.09948*, 2019.
- [38] Nitish Srivastava, Geoffrey Hinton, Alex Krizhevsky, Ilya Sutskever, and Ruslan Salakhutdinov. Dropout: a simple way to prevent neural networks from overfitting. *The journal of machine learning research*, 15(1):1929–1958, 2014.
- [39] Mark Horowitz. 1.1 computing’s energy problem (and what we can do about it). In *2014 IEEE International Solid-State Circuits Conference Digest of Technical Papers (ISSCC)*, pages 10–14. IEEE, 2014.
- [40] Ali Shafiee, Anirban Nag, Naveen Muralimanohar, Rajeev Balasubramonian, John Paul Strachan, Miao Hu, R Stanley Williams, and Vivek Srikumar. Isaac: A convolutional neural network accelerator with in-situ analog arithmetic in crossbars. *ACM SIGARCH Computer Architecture News*, 44(3):14–26, 2016.
- [41] Tianqi Chen, Bing Xu, Chiyuan Zhang, and Carlos Guestrin. Training deep nets with sublinear memory cost. *arXiv preprint arXiv:1604.06174*, 2016.
- [42] Yu-Hsin Chen, Joel Emer, and Vivienne Sze. Eyeriss: A spatial architecture for energy-efficient dataflow for convolutional neural networks. *ACM SIGARCH Computer Architecture News*, 44(3):367–379, 2016.